Biophysical Chemistry 150 (2010) 129–135

Contents lists available at ScienceDirect

Biophysical Chemistry

journal homepage: http://www.elsevier.com/locate/biophyschem

Packing behaviour of two predominant anionic phospholipids of bacterial cytoplasmic membranes ☆

Florian Prossnigg, Andrea Hickel [1], Georg Pabst, Karl Lohner *

Institute of Biophysics and Nanosystems Research, Austrian Academy of Sciences, Schmiedlstrasse 6, A-8042 Graz, Austria

ARTICLE INFO

Article history:
Received 24 March 2010
Received in revised form 7 April 2010
Accepted 8 April 2010
Available online 22 April 2010

Keywords:
Phase diagram
Liposomes
Membrane mimics
S. aureus
X-ray diffraction
Differential scanning calorimetry

ABSTRACT

Phosphatidylglycerol and cardiolipin represent the most abundant anionic phospholipid components of cytoplasmic bacterial membranes and thus are used as constituents for membrane mimetic systems. In this study, we have characterized the temperature dependent phase behaviour of the binary system dipalmitoyl-phosphatidylglycerol (DPPG) and tetramyristoyl-cardiolipin (TMCL) using microcalorimetry and X-ray scattering techniques. Both lipids exhibited a very similar main transition temperature (~41 °C), showing a minimum (39.4 °C) for the binary mixtures at $X_{DPPG} = 0.8$, and exhibited low-temperature phase transitions, which were abolished by incorporation of small amounts (≤10 mol%) of the other lipid component. Therefore, over a wide temperature and composition range a lamellar L_{β} gel phase is the predominant structure below the chain melting transition, characterized by a relatively broad wide-angle peak for $X_{DPPG} \leq 0.8$. This observation suggests the existence of packing inconsistencies of the TMCL/DPPG hydrocarbon lattices in the gel phase, supported by the small average size of lipid clusters (~50 lipids) within this composition range. The bilayer thickness for the lamellar-gel phase showed a monotonic increase (56 Å for TMCL to about 58 Å for $X_{DPPG} = 0.8$ at 30 °C), which may be explained by different degrees of partial interdigitation of the acyl chains to compensate for the differences in the hydrocarbon lengths of DPPG and TMCL in the L_{β} phase.

1. Introduction

We face a worldwide increase in pathogenic bacteria that are (multi-)resistant to commercially available antibiotics, while the number of novel antibiotics on the market declines. Several strategies to retrieve control on bacterial infections have been developed in the last decade (e.g. Lohner [1]). One promising approach is based on antimicrobial peptides. They mostly perturb and destroy the structural integrity of the lipid membrane, although some of these peptides seem to pass the membrane barrier and to act on cytosolic targets [2,3]. Of particular interest is in any case the cell specificity of antimicrobial peptides, i.e. to discriminate between the host and bacterial cell membrane. While the outer leaflet of mammalian plasma membranes almost exclusively consists of neutral phospholipids, the bacterial one has a high content of negatively charged phospholipids, which is supposed to be a predominant factor for the affinity of the positively charged peptides to bacterial membranes. However, recently we showed that in respect of membrane-perturbing mechanism lipid net charge is not the decisive factor, but lipid packing density, the ability to form intermolecular H-bonds and lipid molecular shape have to be also taken into account [4]. Therefore, it is of interest to study the properties of membrane mimetic systems such as structure or packing properties.

As indicated above bacterial cell membranes have high contents of negatively charged lipids like phosphatidylglycerol (PG) or diphosphatidylglycerol (DPG or cardiolipin), which are the most abundant anionic phospholipids of cytoplasmic bacterial membranes. These phospholipids are particularly prominent in a number of Gram-positive bacteria (Table 1). Interestingly, the level of cardiolipin may substantially be increased under certain environmental (e.g. high salt) or stress conditions as reported for *S. aureus* [5–8]. The increased amount of cardiolipin may reflect a requirement for enhancement of the structural integrity of the bacterial cell membrane or for the support of stress-related increases in energy transduction, or both [5,9].

Cardiolipin with its quadruple hydrocarbon chains is a unique lipid also found in a significant amount in the inner mitochondrial membrane

Abbreviations: DPG, diphosphatidylglycerol (cardiolipin); TMCL, tetramyristoyl-cardiolipin; (DP)PG, (dipalmitoyl-)phosphatidylglycerol; PE, phosphatidylethanolamine; $L_{c'}$, subgel phase; SGII, subsubgel phase with tilted hydrocarbons; L_{R1}, subsubgel phase with untilted hydrocarbons; L_{β}, lamellar-gel phase with untilted hydrocarbon chains; $L_{\beta'}$, lamellar-gel phase with tilted hydrocarbon chains; $P_{\beta'}$, ripple-gel phase; L_{α}, fluid phase with melted hydrocarbon chains; DSC, differential scanning calorimetry; $T_{(m)}$, (main) transition temperature; T_{pre}, pre-transition temperature; $\Delta H_{(m)}$, (main) transition enthalpy; ΔH_{pre}, pre-transition enthalpy; SWAXS, small and wide-angle X-ray scattering; z_H, distance between head group and centre of the bilayer; d_B, thickness of the bilayer; OLV, oligolamellar vesicles; X_{DPPG}, mol fraction of DPPG.

☆ Dedicated to Prof. Dr. Alfred Blume on the occasion of his 65th birthday.

* Corresponding author. Tel.: +43 316 4120 323; fax: +43 316 4120 390.
E-mail address: karl.lohner@oeaw.ac.at (K. Lohner).
[1] Present address: Chemie-Ingenieurschule Graz, Triester Straße 361-361a, A-8055 Graz, Austria.

0301-4622/$ – see front matter © 2010 Elsevier B.V. All rights reserved.
doi:10.1016/j.bpc.2010.04.004

Table 1
Membrane phospholipid composition of representative Gram-positive bacteria (see K. Lohner [38] and references therein).

Bacteria species	Phospholipid as percentages of the total				
	PG[a]	Cardiolipin	Lysyl-PG	PE	Others
Staphylococcus aureus	57	5	38	0	Trace
Bacillus subtilis	29	47	7	10	6[b]
Micrococcus luteus	26	67	0	0	7[c]

[a] PG, phosphatidylglycerol; PE, phosphatidylethanolamine.
[b] Including phosphatidic acid and glycolipids.
[c] Almost exclusively phosphatidylinositol.

of eukaryotic cells being essential for e.g. insertion and translocation of proteins in the inner mitochondrial membrane [10]. While it seems that a major biological role of cardiolipin is related to the function of membrane proteins [9], Haines and Dencher [11] suggested another important function for cardiolipin due to its high pK_{a2} value (>8), which enables cardiolipin to trap protons at the H^+-uptake pathway of the energy transducing membrane [for details see [12]]. PG does not show such a variety of specific functions, but serves as precursor molecule for the biosynthesis of cardiolipin and other phospholipid molecules [13].

Regarding bacteria, cardiolipin was described to be concentrated in polar and septal regions as visualized by nonyl acridine orange (see Mileyovskaya [14], Schlame [15], and references therein). The ability to form non-lamellar structures is supposed to be required for membrane curvature in the septal region of cytoplasmic membranes, which is related to the cell division process. The propensity to form non-lamellar structures is referred to the small polar head group of cardiolipin (see Matsumoto [16] and references therein). Because of this unique conformation, this lipid is also able to pack tightly forming micro domains [11] and in stack like arrays, which are also stabilized by membrane proteins [16]. Haines et al. [11] described the head group as a bicyclic formation of the two phosphate groups linked to the centred glycerol residue. Thereby, the H-bonding to the hydroxyl residue alters the pK_a to >8 and creates – by trapping a proton – an acid-anion. Therefore, at physiological conditions, cardiolipin has a single negative charge on the head group [11]. PG also carries one net negative charge at physiological pH (pK_a value of ~3 [17,18]), but unlike cardiolipin the cross section of the head group is comparable to the cross section of its hydrocarbon chains. This gives the lipid a cylindrical molecular shape and thus PG will prefer to form flat bilayers.

Although there is a wealth of knowledge on the individual lipids, to our knowledge no study has been reported so far on binary mixtures of PG and cardiolipin, which represents an interesting model system for some Gram-positive cytoplasmic membranes. As lipids we have chosen the saturated species dipalmitoyl-PG (DPPG) and tetramyristoyl-cardiolipin (TMCL). The thermotropic phase behaviour of both lipids has been characterized showing very similar chain melting transition (around 41 °C) under comparable buffer conditions [19,20]. Moreover, both lipids are characterized by a similar membrane hydrophobic core in the lamellar-gel phase, which can be explained by the chain tilt of DPPG that compensates for its longer chain length (C16 vs. C14) as shown in this study. The experiments were performed at physiologically relevant buffer conditions using differential scanning calorimetry (DSC) and small and wide-angle X-ray scattering (SWAXS) techniques to yield thermodynamic and structural parameters of the DPPG/TMCL mixture.

2. Materials and methods

2.1. Preparation of liposomes

1,2-dipalmitoyl-phosphatidylglycerol (DPPG) and tetramyristoyl-cardiolipin (TMCL) were obtained from Avanti Polar Lipids Inc. (Alabaster, AL, USA) as Na-salt powders and used without further purification. Stock solutions were prepared by dissolving the required amounts of DPPG or TMCL in chloroform/methanol, 2/1 (vol/vol). For film preparation, mixtures of calculated stock solution quantities were evaporated under a nitrogen gas stream and at a temperature of 40 °C until a thin lipid film remained. The films were kept under vacuum over night for total solvent evaporation. The hydration procedure comprised an incubation time of 90 min at 65 °C, interrupted by thorough vortex mixing. The hydration buffer consisted of 20 mM NaPi, pH 7.4, 130 mM NaCl prepared from highly purified water (Milli-Q water purification system).

2.2. Differential scanning calorimetry

Differential scanning calorimetry (DSC) measurements were performed with a VP-DSC high-sensitivity calorimeter from MicroCal, LLC (Northampton, MA, USA). The lipid concentration was 1 mg/ml. At least two sample preparations were performed for each mixture to check on repeatability. Prior to experiments, all samples were degassed for 5 min at room temperature. The scanning temperature range was set between 1 and 60 °C and the scan rate was adjusted at 30 °C/h. The equilibration time before each scan was 15 min. For each measurement the scan program included three heating/cooling cycles showing identical thermograms for the second and third scans, which were used for data evaluation. This was performed with Origin 7 SR4 including a calorimetric modelling package. Recorded DSC thermograms were normalized with respect to the lipid concentration and scan rate. After baseline correction, the calorimetric enthalpies (ΔH) were determined by integrating the peak areas. The calorimetric enthalpy, the maximum heat capacity and the phase transition temperature were used for calculation of the van't Hoff enthalpy [21,22] in order to calculate the cooperativity of the main transition given by the ratio between van't Hoff and calorimetric enthalpy.

2.3. X-ray scattering

Small and wide-angle X-ray scattering (SWAXS) patterns were recorded on a SWAX camera (System 3, Hecus X-ray Systems, Graz, Austria) using a sealed X-ray tube generator from Seifert (Ahrensburg, Germany) working at 50 kV and 40 mA. The X-ray beam was filtered for CuK_α radiation ($\lambda = 1.542$) using a Ni foil and a pulse height discriminator. The SWAXS patterns were recorded in the wave vector ($q = 4\pi\sin\theta/\lambda$, where θ is half the scattering angle) regimes of 10^{-3} Å$^{-1} < q < 1$ Å^{-1} (SAXS) and 1.2 Å$^{-1} < q < 2.7$ Å^{-1} (WAXS) using two linear, one-dimensional, position-sensitive detectors (PSD 50, Hecus X-ray Systems, Graz, Austria). Silver stearate and p-bromo-benzoic acid were used for detector calibration of the small and the wide-angle range, respectively. Temperature was controlled with a Peltier heating unit.

Lipid samples (concentration 50 mg/ml) were filled into thin walled 1 mm capillaries (Hilgenberg GmbH, Malsfeld, Germany) and sealed with a two-component adhesive. To prevent sedimentation, the capillaries were rotated at constant speed along their axis within the sample stage. Data sets of pure buffer solution were recorded at 25 °C and used for baseline subtraction. Background corrected SAXS data were evaluated in terms of the Global Analysing Program developed by Pabst et al. [23,24]. In the applied model, the bilayer electron-density profile is given by the summation of three Gaussian distributions, two describing the electron-density of the head group region and one at the centre of the bilayer accounting for the minimum density at the methyl terminus of the hydrocarbon chains.

The main parameters determined by SAXS data evaluation are the distance between head group and centre of the bilayer (z_H), the hydrocarbon chain length and the thickness of the bilayer (d_B), respectively, which were determined as detailed previously [25]. Peak

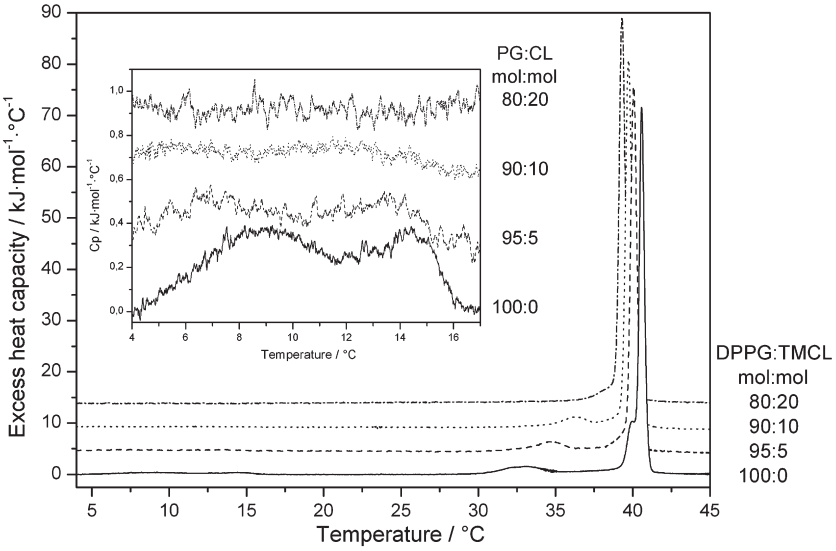

Fig. 1. Selected thermograms of the DPPG enriched region of binary mixtures of DPPG/TMCL at a scan rate of 30 °C/h. Inset shows the subsubgel to lamellar-gel phase transition region. Molar ratios of the binary mixtures are indicated in the panel.

positions in recorded WAXS patterns are fitted by Gaussians to determine the hydrocarbon chain lattice.

3. Results and discussion

The thermotropic phase behaviour of both lipids, DPPG and TMCL, has been well documented previously [19,20,26,27]. In accordance with published data the endotherm of pure DPPG liposomes showed two clearly discernable transitions (Fig. 1, Table 2), which can be attributed to the pre-transition from the lamellar-gel (L_{β}') to the ripple phase (P_{β}') at 33.2 °C and the main or chain melting transition from the P_{β}' to the fluid (L_{α}) phase at 40.7 °C. In addition, two overlapping weak enthalpic transitions were observed with transition temperatures of 9.2 and 14.4 °C, respectively. These transitions can be attributed to the subsubgel SGII to $L_{\beta 1'}$ transition, also known as the Y-transition [28] and the head group tilt transition from $L_{\beta 1'}$ to $L_{\beta 2'}$ [27]. The SGII phase has been described as a highly compact metastable gel phase with the tilted hydrocarbon chains, packed on an orthorhombic lattice of two-nearest-neighbour type [28]. The $L_{\beta 1'} \rightarrow L_{\beta 2'}$ transition, in turn, is due to tilt of the PG head group away from the nearly horizontal position, because of lateral hydrocarbon chain pressure [27]. For TMCL it was shown that upon long-term incubation at low temperatures (−20 °C overnight) this lipid adopts a stable subgel $L_{c'}$-phase, which transforms into a L_{β} phase upon heating between 25 and 29 °C depending on the buffer used [20]. This phase transition exhibits a pronounced cooling hysteresis and is not completed during a simple cooling scan and therefore upon immediate reheating two low-temperature endothermal peaks between 14–18 °C and 25°–30 °C were reported [20]. This is the situation applied in our experiments and thus, in excellent agreement with these earlier findings using a similar phosphate buffer containing EDTA, we also observed two endothermic low-temperature transitions at 17.9 °C and 27.7 °C, respectively, as well as the main transition at 40.9 °C (Fig. 2, Table 2).

A biphasic behaviour was observed for the main transition temperature of the binary mixtures (Table 2). Adding DPPG to TMCL resulted at first in a monotonic decrease of the main transition temperature until a molar ratio of DPPG/TMCL 80/20 and in a monotonic increase upon further addition of DPPG (39.4 °C as compared to 40.9 °C for TMCL and 40.7 °C for DPPG). Similarly, the cooperativity of the main transition, which is a measure for the size of the average lipid domain undergoing the gel-fluid transition, showed also a biphasic behaviour with a breakpoint around $X_{DPPG} = 0.8$. An average cluster size of about 50 lipids was calculated within the composition range of $X_{DPPG} \leq 0.8$, which corresponds to the value calculated for pure TMCL, while at higher DPPG content the cooperativity increased with an average cluster size of 180 lipids calculated for DPPG. Unlike, these two parameters, the main transition

Table 2
Phase transition temperatures and enthalpies for binary mixtures of DPPG/TMCL.

	Low-temperature transitions				Pre-transition		Main transition	
	SGII/$L_{R1} \rightarrow L_{\beta}'$	ΔH	$L_{c'} \rightarrow L_{\beta}$	ΔH	$L_{\beta}' \rightarrow P_{\beta'}$	ΔH_{pre}	$L_{\beta}/P_{\beta}' \rightarrow L_{\alpha}$	ΔH_m
X_{DPPG}	T [°C]	kJ mol^{-1}	T [°C]	kJ mol^{-1}	T_{pre} [°C]	kJ mol^{-1}	T_m [°C]	kJ mol^{-1}
1	9.2/14.4	2.3			33.2	5.8	40.7	38.6
0.95	7.5/13.1	~1.5			34.7	6.4	40.2	43.6
0.9	5.9/11.8	~0.5			36.5	5.9	39.9	42.8
0.8							39.4	48.2
0.7							39.4	51.7
0.6							39.8	47.9
0.5							39.9	51.1
0.4	7.7	1.1					40.1	53.5
0.3	10.8	4.8					40.3	54.4
0.2	13.4	8.6					40.6	54.6
0.1	15.3	13.0	24.1	1.3			40.6	55.8
0	17.9	10.4	27.7	23.8			40.9	55.5

Phase designation see text.

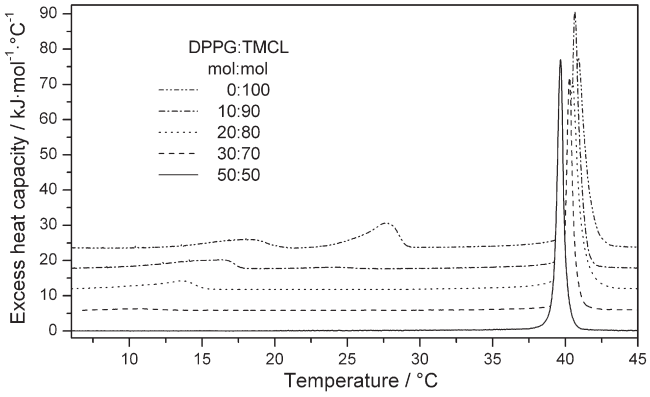

Fig. 2. Selected thermograms of binary mixtures of DPPG/TMCL ($X_{DPPG} \leq 0.5$) at a scan rate of 30 °C/h. Molar ratios of DPPG/TMCL are indicated in the panel.

enthalpy showed a non-monotonic decrease from 55.5 kJ/mol for pure TMCL to 38.6 kJ/mol for pure DPPG (Table 2). However, considering the different numbers of hydrocarbon chains linked to the glycerol moiety of the two lipids and their respective impact on the chain melting process suggests to plot the main transition enthalpy with respect to the ratio of number of acyl chains. This graph then shows that the main transition enthalpy follows a linear dependence (Fig. 3).

A different behaviour was observed for the low-temperature transitions of the individual lipids, which in general were rapidly abolished upon admixture of the other lipid component (Figs. 1, 2; Table 2). The low-temperature transition of pure TMCL with corresponding values of 27.7 °C and 23.8 kJ/mol, characteristic for the transformation of the $L_{c'}$- into the L_{β}-phase, was hardly discernible from the baseline when 10 mol% of DPPG was added (24.1 °C, 1.3 kJ/mol). On the other hand, the second low-temperature transition observed for TMCL at 17.9 °C persisted up to 40 mol% DPPG under the given experimental conditions, whereby the corresponding transition temperatures and enthalpies decreased monotonically with the admixture of DPPG from $T = 17.9$ °C and $\Delta H = 10.4$ kJ/mol (pure TMCL) to $T = 7.7$ °C and $\Delta H = 1.1$ kJ/mol ($X_{DPPG} = 0.4$), respectively. Within the composition range of $0.5 \leq X_{DPPG} \leq 0.8$ no low-temperature phase transitions were observed. For $X_{DPPG} \geq 0.9$ weak double peaks at 9.2 °C and 14.4 °C, similar to pure DPPG dispersions were observed, which we therefore ascribed analogously to the head group tilt and Y-transitions [27,28]. In the same DPPG concentration range the pre-transition temperature increased from 33.2 °C for pure DPPG to

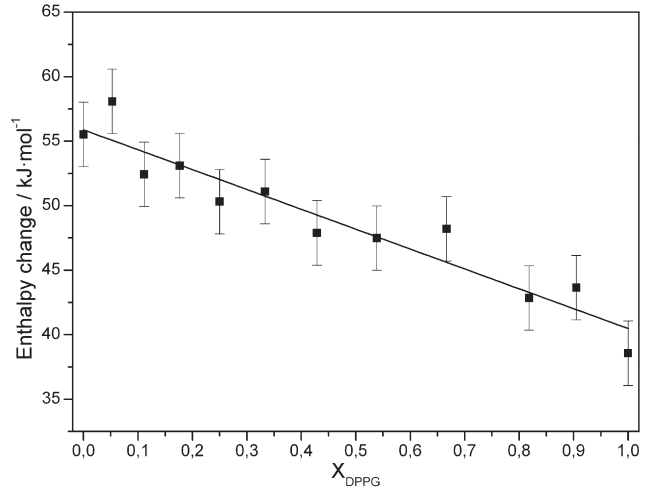

Fig. 3. Main transition enthalpy of binary mixtures of DPPG/TMCL plotted with respect to the ratio of C16/C14 hydrocarbon chains.

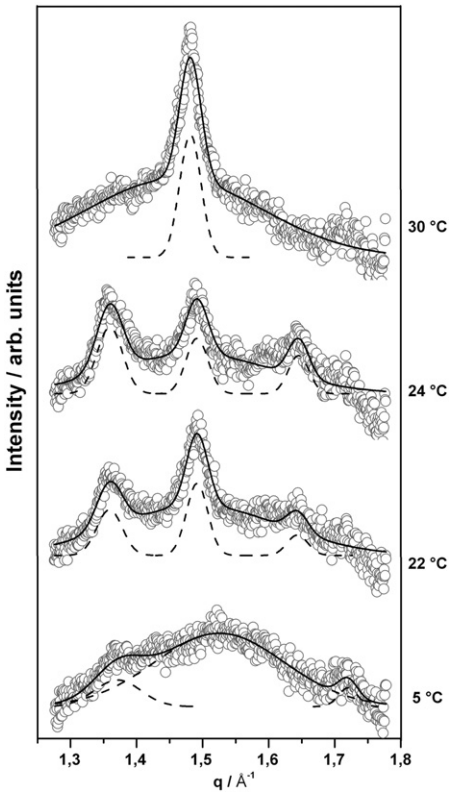

Fig. 4. WAXS patterns of TMCL recorded at 5, 22, 24 and 30 °C, respectively. Open circles show experimental data points, dashed lines represent Gaussian peak fit and solid line is the sum of the fit, showing that in the low-temperature range the WAXS pattern can be described by a superposition of different phases (for details see text).

36.5 °C ($X_{DPPG} = 0.9$) without significant changes in the enthalpy (Fig. 1, Table 2) reflecting a stabilization of the $L_{\beta'}$ phase by adding TMCL to DPPG.

The corresponding individual membrane structures were deduced from X-ray scattering experiments. Fig. 4 shows the wide-angle pattern of pure TMCL below the main transition. The pattern at 5 °C was characterized by a very broad peak with a maximum around $d \sim 4.1$ Å, and small peaks at lower ($d \sim 4.59$ Å) and higher angle ($d \sim 3.66$ Å), whereby $d = 2\pi/q$. The two sharp peaks are close to the positions reported for the $L_{c'}$ phase in TMCL [20]. On the other hand, based on the observations by Tenchov et al. [28] in phosphatidylethanolamines and the present experimental protocol, the two peaks could also originate from a L_{R1} phase. Similar to the SGII phase found in pure DPPG in the present study, the L_{R1} phase describes a highly compact gel phase, but with untilted hydrocarbon chains arranged on an orthorhombic lattice of four-nearest-neighbour type [28]. The broad peak indicates the presence of a domain with weak positional correlations of the acyl chains. Also Lewis et al. [20] described a metastable gel phase in TMCL of relatively small crystalline domains. This is in agreement with our observation, because the peak width scales inversely with the lateral domain size. Once the temperature was increased to 22 °C, i.e. above the lowest phase transition, three clearly resolved Bragg peaks were detected. Thereby, the peaks at $d = 4.62$ Å and $d = 3.85$ Å, respectively, are characteristic for the 2D rectangular lipid arrangement of a well formed $L_{c'}$ phase, while the rather symmetric peak at $d = 4.22$ Å is indicative for a lamellar L_{β} gel phase. This shows that the $L_{c'}$ phase is now coexisting with a well ordered lamellar-gel phase with untilted hydrocarbon chains. Increasing slightly the temperature up to 24 °C, shows relative increase of the peak intensities of subgel phase with respect to the L_{β} phase. Heating further to 30 °C we observed a single symmetric peak in the WAXS pattern demonstrating the existence of a single

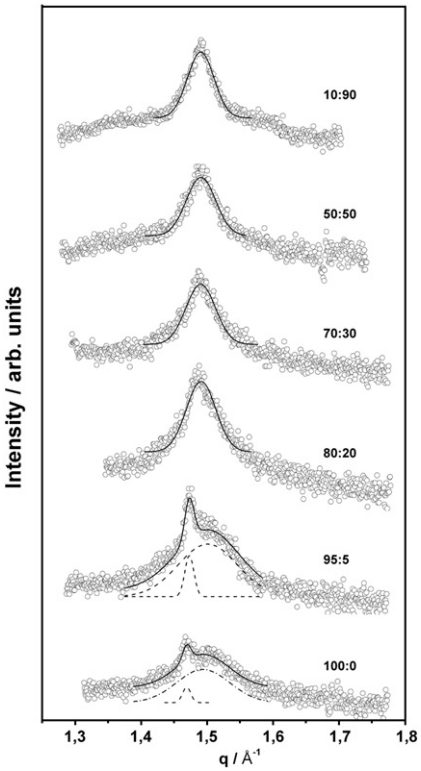

Fig. 5. WAXS patterns of selected DPPG/TMCL mixtures recorded at 22 °C (molar ratio indicated in the panel). Open circles show experimental data points, dashed lines represent Gaussian peak fit and solid line is the sum of the fit.

L_{β}-gel phase. The L_{β} phase expanded laterally with increasing temperature as indicated from the change of the WAXS peak from $d = 4.21$ Å at 30 °C to $d = 4.28$ Å at 37 °C. The wide-angle data of pure DPPG were typical for an $L_{\beta'}$ phase at low temperatures (sharp d_{20} and broad d_{11} peak) and showed a single broad peak in the $P_{\beta'}$ phase in agreement with previous reports [27] (Fig. 5).

Mixtures of TMCL and DPPG have to accommodate the different packing properties of the individual lipid species. At 22 °C, i.e. above the second phase transition of TMCL, already 10 mol% of DPPG suffices to practically abolish the subgel phase. The WAXS patterns show a single peak centred at $d = 4.21$ Å, a situation which persists up to TMCL:DPPG molar ratios of 20:80 (Fig. 5). The peak width is rather broad and compares to the one of the $P_{\beta'}$ phase of pure DPPG. SAXS data, however, show no indications for a ripple phase, but peaks that index on a single lamellar lattice (Fig. 6). Thus, for $0.1 < X_{DPPG} \leq 0.8$ the TMCL:DPPG forms a lamellar L_{β} phase. The extended peak width indicates packing inconsistencies of the TMCL/DPPG hydrocarbon chain lattices. A sharp d_{20} and a broad d_{11} reflection, characteristic for $L_{\beta'}$ phases, are observed for $X_{DPPG} \geq 0.85$ (Fig. 5). Thus, the four hydrocarbons of TMCL quickly diminish the $L_{\beta'}$ phase upon its addition to DPPG. A very similar situation is also observed at 30 °C, i.e. the WAXS pattern exhibited the same shape and width as compared to the pattern recorded at 22 °C. Thus, for $0 \leq X_{DPPG} \leq 0.8$ we found a loosely packed untilted lamellar L_{β} gel phase, while tilted hydrocarbon chains dominate the $L_{\beta'}$ gel phase at higher DPPG content. Fig. 7 shows the corresponding peak positions. The transition from loosely packed L_{β} to well ordered $L_{\beta'}$ agrees with our DSC results on the cooperativity (see above). Hence, TMCL, over a large concentration range dominates the acyl chain packing in the gel phase.

Interestingly, untilting of the hydrocarbon chains by addition of TMCL to DPPG does not lead to an increase of the membrane thickness, as derived from fits to the SAXS data (Fig. 6). The bilayer thickness rather remains constant at $d_B = 57.9 \pm 0.3$ Å for $X_{DPPG} \geq 0.8$

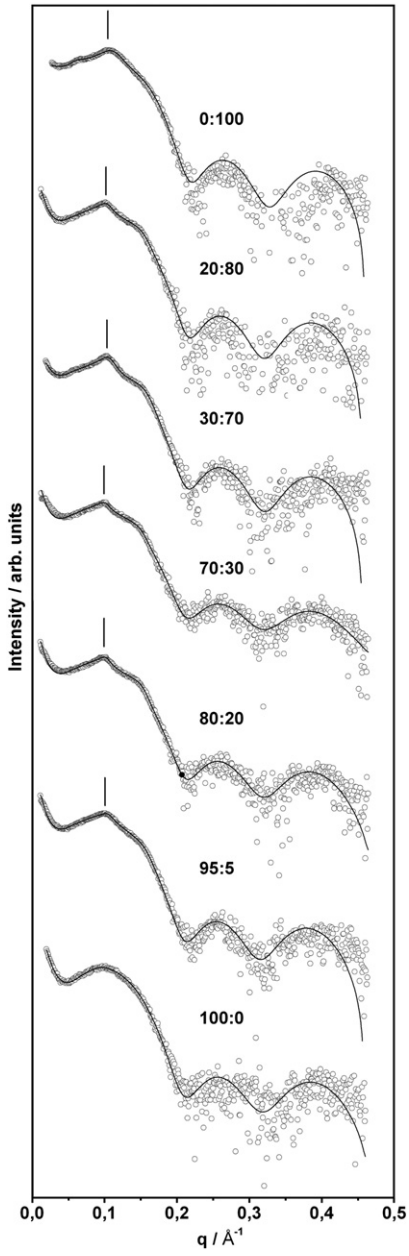

Fig. 6. SAXS patterns in the lamellar-gel phase at 30 °C for the binary system DPPG/TMCL (molar ratio is indicated in the panel). Open circles represent experimental data points and solid lines give the best fit of the global analysis model to the scattered intensities. Position of the second order reflection of the pseudo-Bragg peak for oligolamellar vesicles is indicated in the panel.

and then decreases monotonically to $d_B = 56.0 \pm 0.3$ Å, the final value of pure TMCL (Fig. 8). The constant bilayer thickness above 80 mol% DPPG, correlates with the occurrence of the $L_{\beta'}$-phase within this composition and temperature range and suggests that small amounts of TMCL can be incorporated within this phase without markedly affecting the tilt angle of the acyl chains. The decease of d_B, which is paralleled by the removal of the chain tilt by TMCL at lower DPPG concentration, may be explained by a partial interdigitation of the longer (C16) acyl chains of DPPG with the shorter (C14) acyl chains of TMCL to compensate for the difference of two methylene groups. This would also account for the packing problems and the correlated low melting cooperativity in this concentration regime.

The SAXS data also revealed that incorporation of TMCL affects the lamellarity of the liposomes formed (Fig. 6). SAXS patterns

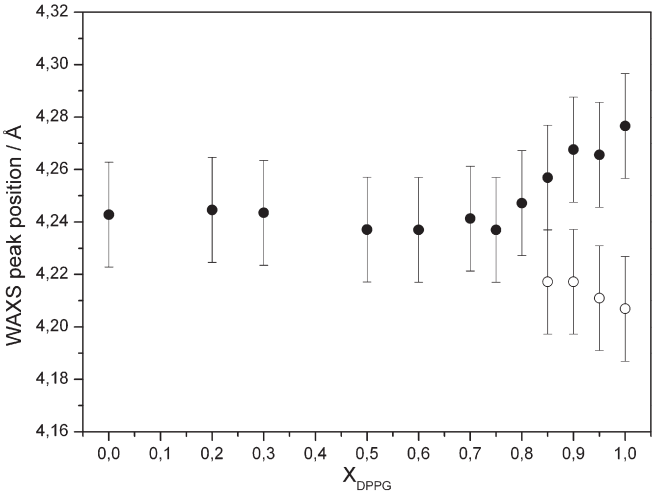

Fig. 7. Position of the Bragg peaks of the wide-angle pattern of binary mixtures of DPPG/TMCL recorded at 30 °C. Within the composition range of $X_{DPPG} \leq 0.8$ the samples adopt a L_{β} phase. At higher DPPG content a $L_{\beta'}$ phase was detected (full circles correspond to the sharp d_{20} peak and open circles to the broad d_{11} peak).

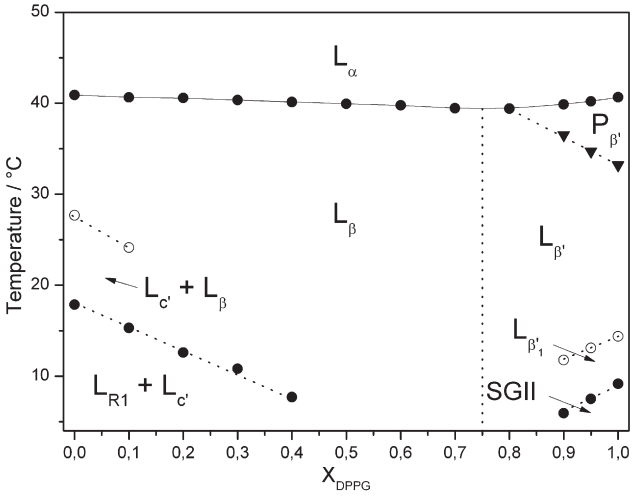

Fig. 9. Schematic phase diagram of the binary system DPPG/TMCL under physiological buffer condition (130 mM NaCl, 20 mM NaPi, pH 7.4) established from DSC experiments. Phase assignment was performed by SWAX experiments: metastable subgel phase, L_{R1}; subgel phase, $L_{c'}$; subsubgel phase, SGII; lamellar-gel phase with tilted, $L_{\beta'}$, and untilted hydrocarbon chains, L_{β}; ripple-gel phase, $P_{\beta'}$, and fluid phase with melted hydrocarbon chains, L_{α}.

recorded for pure DPPG were typical for unilamellar vesicles or positionally uncorrelated bilayers (absence of Bragg peaks). However, after admixture of TMCL, pseudo-Bragg peaks were detected in the SAXS patterns characteristic for oligolamellar vesicles (OLVs) as observed e.g. for anionic/zwitterionic PG/PE mixtures [29]. The formation of oligolamellar vesicles depends on the balance of attractive (van der Waals) and repulsive (hydration, steric, electrostatic) forces. Latter are strongly influenced by both the composition of the buffer and the charge of the lipid head groups. A decrease or a shielding of the surface net charge causes decreased repulsive forces and consequently the formation of OLVs [30]. This seems to be the case for samples containing TMCL considering that the phosphate residues form a tight bicyclic structure with H-bonds to the hydroxyl group on the centred glycerol [11]. As a consequence one of the acidic protons is trapped in this configuration forming an acid-anion and, in turn, reducing the net charge to −1 at neutral pH instead of −2 as expected from the presence of the two phosphate groups. Taking into account the increased cross sectional area of the TMCL molecule owing to the four hydrocarbon chains this property results in a reduced surface charge density and therefore enables formation of OLVs.

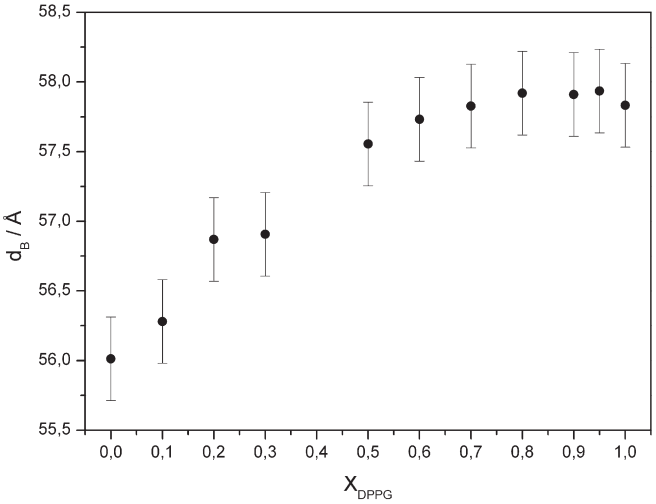

Fig. 8. Bilayer thickness (d_B) of the lamellar-gel phase of binary mixtures of DPPG/TMCL at 30 °C calculated from z_H applying the global analysis model to the scattered intensities (for details see Materials and methods).

4. Schematic phase diagram

A schematic presentation of the phase diagram of the binary mixture of DPPG and TMCL based on their heat capacity functions is given in Fig. 9. Phase assignment, as indicated in the figure, was deduced from the X-ray diffraction data. The phase sequence observed for pure DPPG is indicated in the figure and in agreement with earlier data [27]. Under the experimental protocol used, which did not apply overnight incubation of the samples at −20 °C but only 15 min at 1 °C, TMCL formed a metastable weakly ordered L_{R1} phase [28] that coexisted with the subgel $L_{c'}$ phase at low temperatures. At higher temperatures the $L_{c'}$ phase coexists with the lamellar L_{β} gel phase. As can be deduced from the phase diagram, incorporation of small amounts ($\leq$10 mol%) of one lipid strongly affects the low-temperature phase behaviour of the other lipid component, whereby DPPG prevented the formation of the subgel $L_{c'}$ phase and TMCL abolished the subsubgel (SGII) phase. Thus, over a wide temperature and composition range a lamellar L_{β} gel phase is the predominant structure below the chain melting transition.

The width of the respective wide-angle patterns, which showed no significant changes upon heating or amount of DPPG added, was comparable to the width of the wide-angle pattern obtained for the $P_{\beta'}$ ripple-gel phase. This suggests that the lipid components do not mix ideally in the gel phase, which is supported by the small average lipid cluster size of about 50 lipids calculated for this composition range ($X_{DPPG} \leq 0.8$). Further, the composition dependence of the main transition temperature, showing lower transition temperatures for all binary mixtures with a minimum around $X_{DPPG} = 0.8$, suggests nonideal mixing of the binary components (eutectic mixture). In contrast to the hydrocarbon chain packing, the bilayer thickness was dependent on the molar ratio of the two lipids within this composition range. Adding DPPG to TMCL resulted in a concentration dependent increase of the bilayer thickness by about 2 Å in total, corresponding to the segment of about 2 methylene groups, and reached the value of pure DPPG at $X_{DPPG} = 0.8$. This behaviour may be explained by the need of different degrees of partial interdigitation in the methyl region of the bilayer core to compensate for the differences in the effective hydrocarbon lengths of DPPG and TMCL. Nonideal

miscibility was also reported for another binary mixture being of relevance for bacterial membrane mimetic systems, namely phosphatidylglyerol and -ethanolamine [26,29]. In these systems, phase separation of pure components was observed in the gel phase, which was attributed to be mainly due to differences in the head group interactions. In the present case, packing constrains due to different numbers of hydrocarbon chains per lipid have to be overcome and drive the system into a nonideal mixture. Our SAXS data show that pure TMCL membranes are less charged than pure DPPG membranes. Non-random mixing of the two components therefore most likely leads to lateral inhomogeneities of the bilayer charge density. Therefore it will be of interest, to investigate if membrane-active molecules such as antimicrobial peptides can even discriminate between these two anionic lipids. So far, a particular preference of the binding to DPPG head groups compared to cardiolipin was reported for a synthetic antimicrobial hexapeptide [31]. Different binding capabilities to various anionic phospholipids were also demonstrated for the beta-sheet peptide protegrin-1 [32]. Furthermore, lipid demixing has been shown in a number of studies of lipid mixtures being composed of neutral and anionic phospholipids giving rise to the formation of peptide poor and peptide-rich domains [31,33–36]. Lateral phase separation induced by antimicrobial peptides was suggested to have implications on structure and integrity of membranes and may affect adversely the function of membrane proteins [2,37].

Acknowledgement

This work has been supported by the Austrian Science Funds FWF (grant no. P18100-B10 to A.H.).

References

[1] K. Lohner, Development of Novel Antimicrobial Agents: Emerging Strategies, Horizon Scientific Press, Wymondham, 2001.
[2] K. Lohner, S.E. Blondelle, Molecular mechanisms of membrane perturbation by antimicrobial peptides and the use of biophysical studies in the design of novel peptide antibiotics, Comb. Chem. High Throughput Screen. 8 (2005) 241–256.
[3] K. Lohner, New strategies for novel antibiotics: peptides targeting bacterial cell membranes, Gen. Physiol. Biophys. 28 (2009) 105–116.
[4] E. Sevcsik, G. Pabst, W. Richter, S. Danner, H. Amenitsch, K. Lohner, Interaction of LL-37 with model membrane systems of different complexity: influence of the lipid matrix, Biophys. J. 94 (2008) 4688–4699.
[5] H.U. Koch, R. Haas, W. Fischer, The role of lipoteichoic acid biosynthesis in membrane lipid metabolism of growing *Staphylococcus aureus*, Eur. J. Biochem. 138 (1984) 357–363.
[6] F.L. Hoch, Cardiolipins and biomembrane function, Biochim. Biophys. Acta 1113 (1992) 71–133.
[7] Y. Kanemasa, T. Yoshioka, H. Hayashi, Alteration of the phospholipid composition of *Staphylococcus aureus* cultured in medium containing NaCl, Biochim. Biophys. Acta 280 (1972) 444–450.
[8] A. Okabe, Y. Hirai, H. Hayashi, Y. Kanemasa, Alteration in phospholipid composition of *Staphylococcus aureus* during formation of autoplast, Biochim. Biophys. Acta 617 (1980) 28–35.
[9] F.L. Hoch, Cardiolipins and mitochondrial proton-selective leakage, Bioenerg. Biomembr. 30 (1998) 511–532.
[10] K. Matsumoto, Dispensable nature of phosphatidylglycerol in *Escherichia coli*: dual roles of anionic phospholipids, Mol. Microbiol. 39 (2001) 1427–1433.
[11] T.H. Haines, N.A. Dencher, Cardiolipin: a proton trap for oxidative phosphorylation, FEBS Lett. 528 (2002) 35–39.
[12] H. Palsdottir, C. Hunte, Lipids in membrane protein structures, Biochim. Biophys. Acta 1666 (2004) 2–18.
[13] R.P. Huijbregts, A.I. de Kroon, B. de Kruijff, Topology and transport of membrane lipids in bacteria, Biochim. Biophys. Acta 1469 (2000) 43–61.
[14] E. Mileykovskaya, Subcellular localization of *Escherichia coli* osmosensory transporter ProP: focus on cardiolipin membrane domains, Mol. Microbiol. 64 (2007) 1419–1422.
[15] M. Schlame, Cardiolipin synthesis for the assembly of bacterial and mitochondrial membranes, J. Lipid Res. 49 (2008) 1607–1620.
[16] K. Matsumoto, J. Kusaka, A. Nishibori, H. Hara, Mol. Microbiol. 61 (2006) 1110–1117.
[17] A. Watts, K. Harlos, W. Maschke, D. Marsh, Control of the structure and fluidity of phosphatidylglycerol bilayers by pH titration, Biochim. Biophys. Acta 510 (1978) 63–74.
[18] G. Cevc, Membrane electrostatics, Biochim. Biophys. Acta 1031 (1990) 311–382.
[19] G. Degovics, A. Latal, K. Lohner, X-ray studies on aqueous dispersions of dipalmitoyl phosphatidylglycerol in the presence of salt, J. Appl. Crystallogr. 33 (2000) 544–547.
[20] R.N. Lewis, D. Zweytick, G. Pabst, K. Lohner, R.N. McElhaney, Calorimetric, X-ray diffraction, and spectroscopic studies of the thermotropic phase behavior and organization of tetramyristoyl cardiolipin membranes, Biophys. J. 92 (2007) 3166–3177.
[21] P. Garidel, C. Johann, A. Blume, Nonideal mixing and phase separation in phosphatidylcholine-phosphatidic acid mixtures as a function of acyl chain length and pH, Biophys. J. 72 (1997) 2196–2210.
[22] S. Mabrey, J.M. Sturtevant, Investigation of phase transitions of lipids and lipid mixtures by sensitivity differential scanning calorimetry, Proc. Natl. Acad. Sci. U.S.A. 73 (1976) 3862–3866.
[23] G. Pabst, M. Rappolt, H. Amenitsch, P. Laggner, Structural information from multilamellar liposomes at full hydration: full q-range fitting with high quality X-ray data, Phys. Rev., E Stat. Phys. Plasmas Fluids Relat. Interdiscip. Topics 62 (2000) 4000–4009.
[24] G. Pabst, J. Katsaras, V.A. Raghunathan, M. Rappolt, Structure and interactions in the anomalous swelling regime of phospholipid bilayers, Langmuir 19 (2003) 1716–1722.
[25] G. Pabst, A. Hodzic, J. Strancar, S. Danner, M. Rappolt, P. Laggner, Rigidification of neutral lipid bilayers in the presence of salts, Biophys. J. 93 (2007) 2688–2696.
[26] K. Lohner, A. Latal, G. Degovics, P. Garidel, Packing characteristics of a model system mimicking cytoplasmic bacterial membranes, Chem. Phys. Lipids 111 (2001) 177–192.
[27] G. Pabst, S. Danner, S. Karmakar, G. Deutsch, V.A. Raghunathan, On the propensity of phosphatidylglycerols to form interdigitated phases, Biophys. J. 93 (2007) 513–525.
[28] B. Tenchov, R. Koynova, G. Rapp, New ordered metastable phases between the gel and subgel phases in hydrated phospholipids, Biophys. J. 80 (2001) 1873–1890.
[29] B. Pozo-Navas, K. Lohner, G. Deutsch, E. Sevcsik, K.A. Riske, R. Dimova, P. Garidel, G. Pabst, Composition dependence of vesicle morphology and mixing properties in a bacterial model membrane system, Biochim. Biophys. Acta 1716 (2005) 40–48.
[30] B. Pozo-Navas, V.A. Raghunathan, J. Katsaras, M. Rappolt, K. Lohner, G. Pabst, Discontinuous unbinding of lipid multibilayers, Phys. Rev. Lett. 91 (2003) 028101.
[31] A. Arouri, M. Dathe, A. Blume, Peptide induced demixing in PG/PE lipid mixtures: a mechanism for the specificity of antimicrobial peptides towards bacterial membranes? Biochim. Biophys. Acta 1788 (2009) 650–659.
[32] W. Jing, E.J. Prenner, H.J. Vogel, A.J. Waring, R.I. Lehrer, K. Lohner, Headgroup structure and fatty acid chain length of the acidic phospholipids modulate the interaction of membrane mimetic vesicles with the antimicrobial peptide protegrin-1, J. Pept. Sci. 11 (2005) 735–743.
[33] K. Lohner, E.J. Prenner, Differential scanning calorimetry and X-ray diffraction studies of the specificity of the interaction of antimicrobial peptides with membrane-mimetic systems, Biochim. Biophys. Acta 1462 (1999) 141–156.
[34] K. Lohner, A. Latal, R.I. Lehrer, T. Ganz, Differential scanning microcalorimetry indicates that human defensin, HNP-2, interacts specifically with bBiomembrane mimetic systems, Biochemistry 36 (1997) 1525–1531.
[35] R.F. Epand, M.A. Schmitt, S.H. Gellman, R.M. Epand, Role of membrane lipids in the mechanism of bacterial species selective toxicity by two alpha/beta-antimicrobial peptides, Biochim. Biophys. Acta 1758 (2006) 1343–1350.
[36] R.F. Epand, B.P. Mowery, S.E. Lee, S.S. Stahl, R.I. Lehrer, S.H. Gellman, R.M. Epand, Dual mechanism of bacterial lethality for a cationic sequence-random copolymer that mimics host-defense antimicrobial peptides, J. Mol. Biol. 379 (2008) 38–50.
[37] R.F. Epand, R.M. Epand, Lipid domains in bacterial membranes and the action of antimicrobial agents, Biochim. Biophys. Acta 1418 (2009) 97–105.
[38] K. Lohner, Development of novel antimicrobial agents: emerging strategies, in: K. Lohner (Ed.), The Role of Membrane Lipid Composition in Cell Targeting of Antimicrobial Peptides, Horizon Scientific Press, Wymondham, Norfolk, U.K, 2001, pp. 149–156.